EJN fens European Journal of Neuroscience

European Journal of Neuroscience, Vol. 29, pp. 1258–1270, 2009 doi:10.1111/j.1460-9568.2009.06656.x

COGNITIVE NEUROSCIENCE

Contrast independence of cardinal preference: stable oblique effect in orientation maps of ferret visual cortex

Agnieszka Grabska-Barwińska,[1,2,3] Claudia Distler,[4] Klaus-Peter Hoffmann[4] and Dirk Jancke[1,2,3,4]
[1]Cognitive Neurobiology, Ruhr-University Bochum, 44780 Bochum, Germany
[2]International Graduate School of Neuroscience, Ruhr-University Bochum, Bochum, Germany
[3]Bernstein Group for Computational Neuroscience, Ruhr-University Bochum, Bochum, Germany
[4]Department of General Zoology and Neurobiology, Ruhr-University Bochum, Bochum, Germany

Keywords: anisotropy, oblique effect, orientation tuning, striate cortex

Abstract

The oblique effect was first described as enhanced detection and discrimination of cardinal orientations compared with oblique orientations. Such biases in visual processing are believed to originate from a functional adaptation to environmental statistics dominated by cardinal contours. At the neuronal level, the oblique orientation effect corresponds to the numerical overrepresentation and narrower tuning bandwidths of cortical neurons representing the cardinal axes. The anisotropic distribution of orientation preferences over large cortical regions was revealed with optical imaging, providing further evidence for the cortical oblique effect in several mammalian species. Our present study explores whether the dominant representation of cardinal contours persists at different stimulus contrasts. Performing intrinsic optical imaging in the ferret visual cortex and presenting drifting gratings at various orientations and contrasts (100%, 30% and 10%), we found that the overrepresentation of vertical and horizontal contours was invariant across stimulus contrasts. In addition, the responses to cardinal orientations were also more robust and evoked larger modulation depths than responses to oblique orientations. We conclude that orientation maps remain constant across the full range of contrast levels down to detection thresholds. Thus, a stable layout of the functional architecture dedicated to processing oriented edges seems to reflect a fundamental coding strategy of the early visual cortex.

Introduction

Neuronal activity in the early visual cortex co-varies with stimulus attributes such as position, orientation, motion direction, colour and spatial frequency. In a number of carnivores and primates, neurons responsive to these basic cues form overlaid maps in which multiple neuronal selectivities are clustered according to shared preferences (Hubel & Wiesel, 1974; Blasdel & Salama, 1986; Bonhoeffer & Grinvald, 1991; Bosking *et al.*, 1997; Hübener *et al.*, 1997; Xu *et al.*, 2005). The layout of these maps reflects the behavioural importance of available information. For example, the largest region of the cortical retinotopic map processes information about the central portion of the visual field. Likewise it is assumed that the oblique effect, a higher sensitivity to cardinal vs. oblique contours, may encode a bias in environmental information content in that contours of cardinal axes occur more frequently than others (Howard & Templeton, 1966; Appelle, 1972; Leventhal & Hirsch, 1975; Li *et al.*, 2003 for review).

Optical imaging experiments in ferret primary visual cortex were the first to demonstrate orientation map (OM) anisotropies (Chapman & Bonhoeffer, 1998; Coppola *et al.*, 1998a). Vertical and horizontal stimuli evoked the strongest response over large cortical regions, while smaller neuronal populations expressed a preference for oblique orientations. Thereafter, similar anisotropies were also reported for cat area 17 (Wang *et al.*, 2003) and human V1 (Furmanski & Engel, 2000), as well as for higher visual areas (area MT in owl monkey, Xu *et al.*, 2006; cat area 21a, Huang *et al.*, 2006; Liang *et al.*, 2007). Single-cell recordings corroborate the biased distribution of preferred orientations (De Valois *et al.*, 1982; Müller *et al.*, 2000; Li *et al.*, 2003; see Appelle, 1972 for review), and also reveal narrower tuning widths and steeper tuning curves for neurons preferring cardinal orientations (Rose & Blakemore, 1974; Nelson *et al.*, 1977; Orban *et al.*, 1984; Li *et al.*, 2003).

In summary, there is general agreement that the increased proportion of cortical volume devoted to the processing of cardinal orientations is an essential neuronal correlate of the oblique effect.

However, it is still unclear whether the cortical oblique effect remains stable at low contrasts, in particular around the response threshold. By analysing the width of the orientation response function, it was suggested that contrast changes do not affect the orientation tuning of simple cells (Sclar & Freeman, 1982; Skottun *et al.*, 1987; Heeger, 1992; Anderson *et al.*, 2000; Ferster & Miller, 2000; Palmer & Miller, 2007; Finn *et al.*, 2007). Stimulus contrast can, however, influence the shape of orientation tuning curves as

Correspondence: Dr D. Jancke, [1]Cognitive Neurobiology, as above.
E-mail: jancke@neurobiologie.ruhr-uni-bochum.de

Received 17 July 2008, revised 12 January 2009, accepted 12 January 2009

revealed by circular variance (Shapley *et al.*, 2002; Alitto & Usrey, 2004). In fact, such a measure of orientation selectivity has been shown to be inversely dependent on contrast in both simple and complex cells in ferret primary visual cortex (Alitto & Usrey, 2004). Furthermore, the range of amplitudes of contrast responses can vary significantly across cortical neurons (Albrecht & Hamilton, 1982; Sclar *et al.*, 1990). In addition, decreasing stimulus contrast causes a change to a preference for lower temporal frequencies (Holub & Morton-Gibson, 1981; Albrecht, 1995). However, none of the studies tested how preferred orientation correlates with these contrast-related changes in tuning properties. Thus, it cannot be ruled out that around contrast threshold, adaptive mechanisms act unevenly upon neuronal coding of oblique and cardinal orientations, thereby abolishing the oblique effect. Because of their global nature, such mechanisms may remain hidden unless measurements incorporate simultaneous observation of entire cortical areas including large neuronal ensembles. Optical imaging provides the required spatial extent and resolution to investigate potential regrouping within cortical maps. In the present investigation we measured responses to 100% contrast as well as the intermediate contrasts of 30% and 10%, therefore covering the approximate range of the ferret contrast detection as reported by behavioural (Hupfeld *et al.*, 2006) and physiological (Li *et al.*, 2006) studies.

Materials and methods

Experiments were carried out in accordance with the Deutsche Tierschutzgesetz (12 April 2001), the European Communities Council Directive (November 1986, S6 609 EEC), and the NIH guidelines for care and use of animals for experimental procedures, and were approved by the local authorities (Regierungspräsidium Arnsberg). Six ferrets of both sexes (three pigmented, three albinotic, 1–2 years old) were used. In four experiments both hemispheres were measured. The study was designed to test whether albinotic animals may differ in the layout of OMs or in their responses to varying contrast compared with pigmented animals. We found no significant differences between the two phenotypes ($P > 0.1$). The data of both groups were thus pooled. All ferrets had been bred and raised in the animal facility of the Department of General Zoology and Neurobiology, Ruhr-University Bochum in an enriched environment with access to an outdoor enclosure.

After premedication with 0.05 mg/kg atropine sulphate (Braun, Melsungen, Germany), animals were anaesthetized with a mixture of 20 mg/kg ketamine and 2 mg/kg xylazine (Rompun®). Following intratracheal intubation and additional local anaesthesia with bupivacain hydrochloride, animals were placed in a stereotaxic frame and artificially ventilated with air and 0.4–0.6% halothane. Any signs of distress evident in the electrocardiogram were counteracted by immediately increasing the level of halothane. A craniotomy was performed over the occipital region. After dura removal, a chamber of dental acrylic was formed around the opened skull, filled with agar and sealed with a transparent quartz window. During the experiment, the animal was held with an implanted head post and released from the ear bars. After completion of the surgery, paralysis was initiated with alcuronium chloride (Alloferin®) to prevent eye movements. During the entire experiment the heart rate, end-tidal CO_2 and body temperature were monitored and maintained at physiological levels. Additionally, a catheter was introduced into the cephalic vein. During the experiment, the animals received an intravenous infusion of electrolytes (Sterofundin®) and 5% glucose (Braun, Melsungen, Germany) as 2 : 1 containing 0.1 mL/h Alloferin.

Optical recordings

Optical imaging was accomplished using an Imager 3001 (Optical Imaging, Mountainside, NY, USA) consisting of a tandem lens macroscope (Ratzlaff & Grinvald, 1991), 85 mm/1.2 toward camera and 50 mm/1.2 toward subject, attached to a CCD camera (DalStar, Dalsa, Colorado Springs, USA). The camera was focused ~400 microns below the cortical surface to minimize blood vessel artefacts. For detection of intrinsic signals, the exposed cortex was illuminated with red light (605 nm). Data acquisition consisted of 22 frames (400 ms each). Stimulus onset was synchronized with the end of the second frame (800 ms).

Visual stimulation

Stimuli consisted of moving full-field sine wave gratings, 0.2 cycles/°, 7.5 Hz, generated by a stimulus program (VSG Cambridge Research Systems, Rochester, UK), presented with motion direction perpendicular to orientation (0, 45, …, 315°). Additionally, responses to a grey screen (blank) with the same mean luminance (57 cd/m^2) were recorded. Stimuli were displayed on a monitor (120 Hz refresh rate; Trinitron, Sony, Germany), 30 cm in front of the contralateral eye.

Stimulus duration was 8 s. During data acquisition gratings were drifting. During the interstimulus interval (15 s), gratings to be presented in the next data acquisition period were stationary in order to minimize non-selective activation (Bonhoeffer & Grinvald, 1993).

We measured responses to 100%, 30% and 10% grating contrasts. A trial consisted of a series of stimulus presentations. In a given trial, we presented eight full contrast stimuli (100%) as well as eight 30% or eight 10% contrast stimuli, and three blanks. We alternated block-wise (five trials) between trials including either 30% or 10% contrast conditions (referred to as sets of 'HC100%', 'HC30%' or 'LC100%', 'LC10%', respectively, conditions in the text and figures; Supporting information, Fig. S1, depicts an example of all orientation conditions). In order to avoid adaptation effects, 100% and low-contrast gratings were presented consecutively within each trial.

Data analysis

To eliminate high-frequency noise, images were first smoothed with a Gaussian low-pass [$\sigma_L = 2$ pixels (36 microns), filter size = 13 × 13 pixels (0.23 × 0.23 mm^2)]. Subsequently data were normalized by division to the mean activity observed during presentation of blanks and expressed as a fraction of reflectance ($\Delta R/R$). In order to exclude strong vessel artefacts and ongoing slow oscillations in oxygenation levels, we applied a signal-source separation method [generalized indicator function (GIF); Yokoo *et al.*, 2001]. This analysis permits the derivation of adequate parameters for high-pass filter bandwidth without preceding assumptions about the underlying spatial structure of neuronal activity (see Fig. S2 in supporting Appendix S1 for adequate filter size settings and comparison to GIF analysis). The procedure minimizes the trial-wise variability of responses to a given condition, while maximizing the variance of signals collected from different conditions. The GIF analysis performed better than the commonly used principal component analysis (PCA). The GIF analysis was particularly advantageous for the lowest contrast conditions, where PCA components evidently contained a mixture of artefact- and stimulus-related data. Stable cortical maps were obtained between frames 5 and 22 (800–8000 ms after stimulus onset; see Fig. 2).

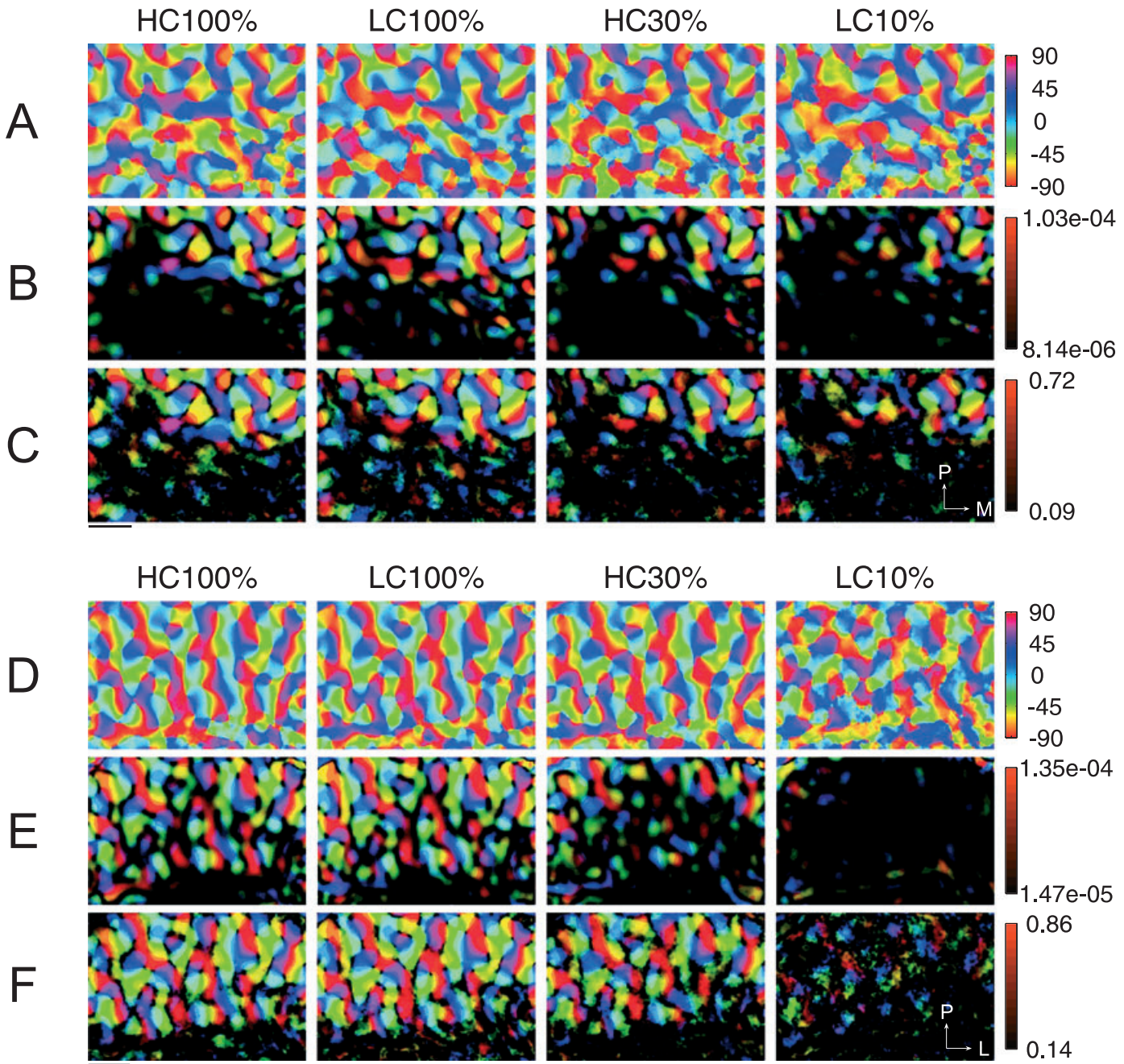

FIG. 1. Contrast dependency of the orientation selectivity arrangement for three types of OMs. Two different experiments are depicted. (A and D) Standard OMs calculated by vector summation, preferred orientation of each pixel is represented by colour. Orientation preference is arranged in pinwheel-like structures that are preserved for all stimulus contrasts but appear more noisy with decreasing contrast. (B and E) Standard polar maps. Hue represents MD, i.e. the length of summation vector (**L**). Maps are clipped to 10–90th percentile, see colour bar for values. MD decreases with decreasing stimulus contrast; cortical regions that revealed high MD in 100% contrast conditions are still prominent at lower contrasts. Dark areas with low MD at the bottom of each image (anterior cortex) represent portions of area 18, brightening towards posterior approximates area 17/18 border. (C and F) Polar maps based on a single (400 ms) frame reproducibility [$r(k, t)$] evaluated across single trials (A–C, 44 HC trials and 46 LC trials; D–F, 22 and 14 trials, respectively). Hue scale represents 10–90th percentile of the values, the theoretically possible reproducibility range is (0, 1). Note that regions of low MD in standard polar maps show increased values in reproducibility polar maps. In particular, maps of 30% and 10% conditions appear brighter in reproducibility polar maps compared with standard polar maps. (D–F) Same experiment as shown in Figs 2 and 3.

Calculation of OMs

OMs (Fig. 1) were calculated by using the filtered single condition maps [high-pass Gaussian, $\sigma_H = 11$ pixels (0.20 mm), filter size = 67 × 67 pixels (1.20 × 1.20 mm^2)] for vector summation (Swindale, 1998):

$$\Phi(k) = \text{angle}(\mathbf{z}(k)) \quad (1)$$

where $\mathbf{z}(k)$ is a complex sum:

$$\mathbf{z}(k) = 1/N\, \Sigma_\varphi\, [f(k, \varphi) \exp\, (i \times 2 \times \varphi)] \quad (2)$$

where $f(k, \varphi)$ stands for the k-th pixel response evoked by a grating moving in the direction φ and N is the number of directions. The

length of the vector sum, $L(k) = |\mathbf{z}(k)|$, defines the orientation modulation depth (MD) and is a common measure of orientation selectivity.

Reproducibility of OMs

Significantly responding cortical regions were detected by calculating the variance across single trials. We defined the reproducibility of the responses (r) as the length of the vector average ($\mathbf{Z}$):

$$r(k) = |\mathbf{Z}(k)| \quad (3)$$

$$\mathbf{Z}(k) = \Sigma_m \exp(i \times 2 \times \Phi(m,k))/M \quad (4)$$

where $\Phi(m, k)$ is the preferred orientation of the k-th pixel in the m-th trial, and M is the number of trials. Consequently, the average angle $\Phi(k) = ½ \text{ angle}(\mathbf{Z}(k))$ is used as the best approximation of the preferred orientation. Furthermore, instead of evaluating the maps across the time-averaged signal, we determined each pixel's reproducibility in each single recording frame (t), and calculated the stable representation of the map by averaging vectors $\mathbf{Z}(k, t)$:

$$\mathbf{Z}'(k) = \Sigma_t[\mathbf{Z}(k,t)/T], \quad (5)$$

where T is the number of summed time frames. Consequently, the stable OMs are calculated as $\Phi'(k) = ½ \text{ angle}(\mathbf{Z}'(k))$, and the reliability as $r'(k) = |\mathbf{Z}'(k)|$.

Pixels consistently reporting similar preferred orientation in various trials were included in regions of interest (ROIs) depending on their reproducibility value. First, for every time frame (t), we calculated the overlap of regions in which reproducibility of orientation preference was higher than r_0 across the various contrast conditions [e.g. $r(k, t) > r_0$ in HC100%, LC100% and HC30%]. Then, the number of frames in which a given pixel responded reliably was compared with the binomial distribution (assuming 50% probability). All significant pixels ($P < 0.01$) were included in the ROI. Finally, the ROI was smoothed with a median filter (9 × 9 pixels; see Carandini & Sengpiel, 2004 for a similar approach). We performed our analysis over a wide range of threshold values ($r_0 = 0.2$ was consistently used for all figures). At this reproducibility threshold ROIs did not contain pixels co-aligned with vessel patterns or pixels located at image corners, and OMs were similar in HC100% and LC100% conditions (see Fig. S3 in supporting Appendix S2 for comparison with the Monte Carlo permutation test). We further verified the results by using subsets of ROIs that did not contain adjacent pixels (minimum distance > 100 microns). With this procedure, first introduced by Müller *et al.* (2000), correlations are decreased due to tissue scattering and low-pass filtering.

Significance tests were performed using Wilcoxon rank-sum test (Matlab statistics toolbox 5.1, The MathWorks; Wilcoxon, 1945). We used this non-parametric test because our data samples were not normally distributed, thus failing to satisfy the assumptions of the commonly used Student's t-test.

Layout of OMs evoked by different stimulus contrasts

To visualize the arrangement of the various orientation-selective domains within a single graph, OMs for each stimulus contrast were calculated using vector summation (Fig. 1A and D). Within the OMs, each colour represents cortical regions containing neurons tuned to a particular orientation.

The OMs obtained for 100% stimulus contrast revealed the typical structure as described earlier (Chapman & Bonhoeffer, 1998; Coppola *et al.*, 1998a; Yu *et al.*, 2005; Li *et al.*, 2006). However, with decreasing contrast (Fig. 1, left to right) the maps became more irregular indicating a decrease in signal-to-noise ratio due to the decline in relative response amplitudes. In order to simultaneously illustrate the MD, we generated standard polar maps (Fig. 1B and E) in which brightness represents orientation strength, i.e. the length (L) of the summation vector. As a typical feature, the resulting polar maps showed low MD around pinwheel centres (Bonhoeffer & Grinvald, 1991). Moreover, the darkening of the images at lower contrast conditions highlights the contrast-dependent decrease in MD across the entire recorded cortical region.

These standard polar maps provide an informative measure of average orientation selectivity at any pixel position. However, they do not allow for a statistical evaluation of the results. Specifically, because our measurements at low stimulus contrasts were performed at response threshold levels, we searched for a way to determine the signal-to-noise ratio inherent to the data. To substantiate the reliability of the underlying cortical responses we therefore introduced another type of polar map (Fig. 1C and F) in which brightness codes for the reproducibility of OMs using orientation selectivity in single trials and in a single time frame. Reliable responses produced less variability over trials and time frames. Thus, the brightest pixels in Fig. 1C and F represent the highest reproducibility values [$r(t)$]. Differences between both types of polar maps are evident in cortical regions with low signal-to-noise ratios due to shallow illumination at image borders (compare upper left and right corners in the two different types of polar maps; Fig. 1E and F). There, activity unrelated to the stimulus led to erroneously high values of vector length in the standard polar maps. Because activity that is not stimulus-locked is variable across trials, our method successfully eliminated those insignificant image pixels. For recordings of high stimulus contrasts, characterized by a high signal-to-noise ratio, both types of polar maps revealed similar results, although high reproducibility values were more evenly distributed across the entire imaged region. Specifically for low-contrast conditions, however, our reproducibility measure assigned significance to regions that displayed low MD in standard polar maps, as evident in the overall brightening of regions containing less prominent vessel artefacts (upper part of the images). In the Supporting information we demonstrate that another approach to estimate signal reliability was less efficient than our method (Monte Carlo permutation test, see Fig. S3 in supporting Appendix S2).

Results

The aim of our study was to investigate the contrast dependence of orientation anisotropies in the visual cortex. To this end we established single condition maps measured for each stimulus orientation and contrast. Sinusoidal gratings of 100%, 30% or 10% contrast were presented moving in eight directions. Figures 2 and 3 show examples measured for cardinally and obliquely oriented stimuli. The maps were obtained by a GIF procedure, which permitted determination of the optimal filter bandwidth applied to subsequent analysis (see Materials and methods and supporting Fig. S1 and, in supporting Appendix S1, Fig. S2). The maps were characterized by a patchy structure that revealed activation of orientation-specific domains (dark pixels).

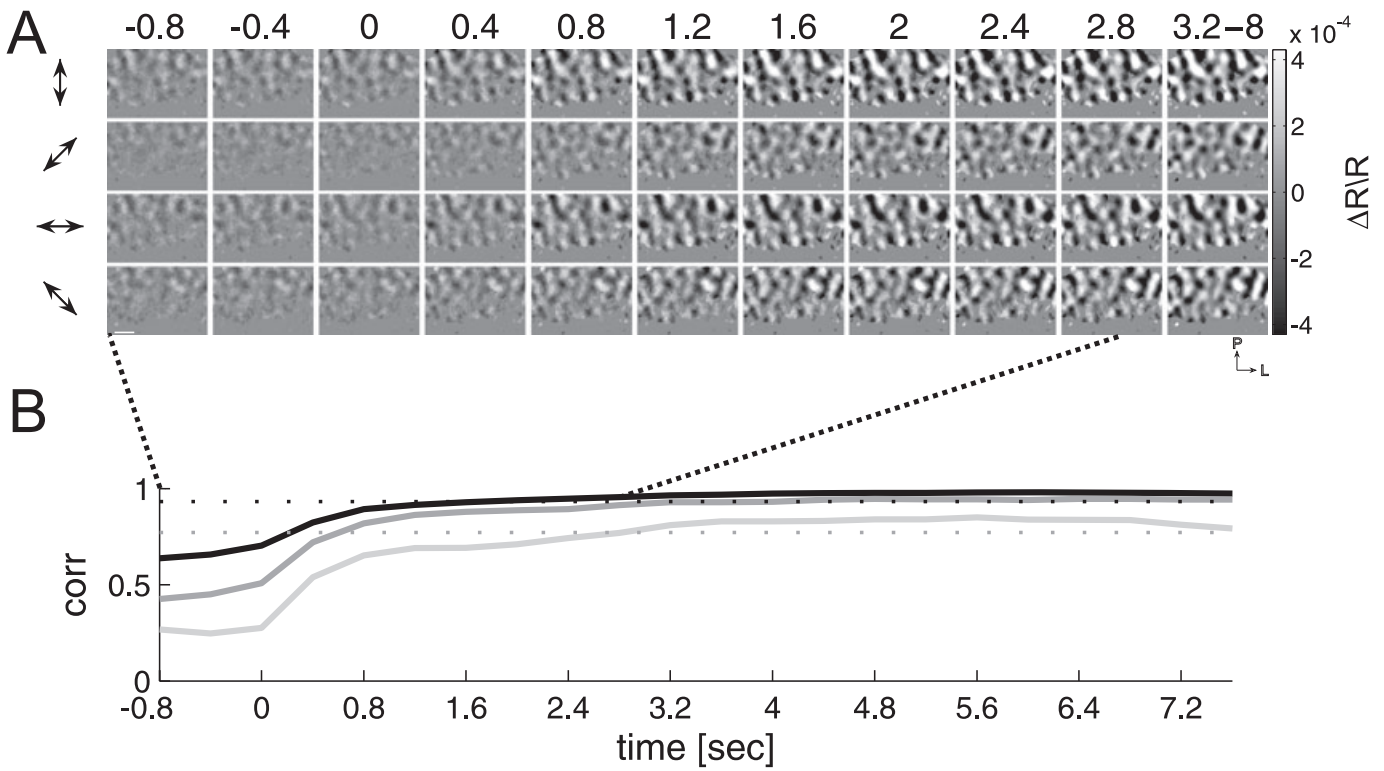

FIG. 2. Emergence and stabilization of single condition OMs. Maps were calculated by a GIF procedure that allowed for the derivation of optimal filter settings (see Materials and methods). The GIF analysis removes common signal components (such as the initial dip, heart beat and respiration-related signals), by minimizing the co-variance between the maps. (A) Time courses of evoked cortical responses to cardinal and oblique orientations, 100% grating contrast (same experiment as in Fig. 1D–F). Pixels that were reliably coding in both 100% and 30% contrast conditions are shown, grey areas mark non-significant pixels. Each frame resolves a 400-ms time window, last column represents time average, 3200–8000 ms. Here and in all figures: P = posterior, L = lateral; horizontal line = 1 mm. (B) Response stability over time. The graphs illustrate correlation coefficients between single time frames and frame average spanning 3200–8000 ms. Correlation coefficients were averaged across orientations (black line = 100%, dark grey = 30%, light grey = 10% contrast; correlations are medians of four ferrets). The correlation value between the two 100% contrast time-averaged maps (3200–8000 ms) recorded in independent HC/LC trials is represented by a black dotted line (c = 0.93). Correlation among 30% and 10% time-averaged maps is depicted by the grey dotted line (c = 0.77). Generally, due to the lower signal-to-noise in low-contrast recordings, correlations across the time-averaged maps were lower for low contrast than for 100% contrast. However, note that correlations of single time frames to the time-averaged maps attained higher values (see intersection with stippled lines around 3.2 s, c = 0.98 for 100%, c = 0.85 for 10%), indicating stable maps after the build-up phase of responses.

Time course of orientation-specific activity

We first examined the time course of the evoked responses by comparing single condition maps in consecutive time frames. Figure 2A presents 400-ms frames of responses measured for 100% contrast in one of the ferrets. Evoked activity in response to oblique and cardinal gratings is depicted for a period of 4 s. The last column depicts the average activity from 3.2 to 8 s. A faint evoked response was visible from the beginning of the recordings followed by a steep signal increase 400–800 ms after stimulus onset (zero). Interestingly, for 100% contrast conditions, orientation-related activity was visible even before the gratings started to move. This most likely resulted from minor activation during pre-stimulus times. A similar lack of adaptation to stationary gratings was observed in single-cell recordings of awake cats (Noda *et al.*, 1971). The presence of small activity patterns at baseline levels rendered them inappropriate as reference frames. We thus omitted the common frame-zero normalization.

The single condition maps derived from orthogonal orientations evoked 'orthogonal' patterns of activity that were stable during the entire phase of the responses (compare dark and bright regions in the first vs. third and the second vs. fourth row, respectively). The response stability over time is summarized by the graphs in Fig. 2B, which depict correlation coefficients derived from comparison of the responses in each single 400-ms time frame with the time-averaged map (last column in Fig. 2A). The graph depicts the median of four cases (two pigmented and two albinotic animals) that showed reliable responses across all contrast conditions. Ten percent contrast did not significantly activate the cortex in the remaining six cases, most probably because this level is within the range of contrast detection threshold in ferrets (Hupfeld *et al.*, 2006).

Correlation coefficients were computed as averages across orientations and are shown separately for each stimulus contrast (darkest line 100%, brightest line 10% conditions). Additionally, to evaluate the variance of the data sets, we calculated correlation coefficients between time-averaged maps evaluated in different subsets of trials. The upper stippled line represents the similarity of 100% HC and 100% LC maps (see also Fig. 3), whereas the lower stippled line indicates the correlation between maps of 30% and 10% conditions.

It can be seen that approximately 800 ms after stimulus onset, activity patterns in response to the entire set of stimulus contrasts became strongly correlated with the averaged maps and remained stable during the rest of the recording period. Thus, for further analysis of OMs, we used imaging frames recorded during the most informative 800–8000-ms time window.

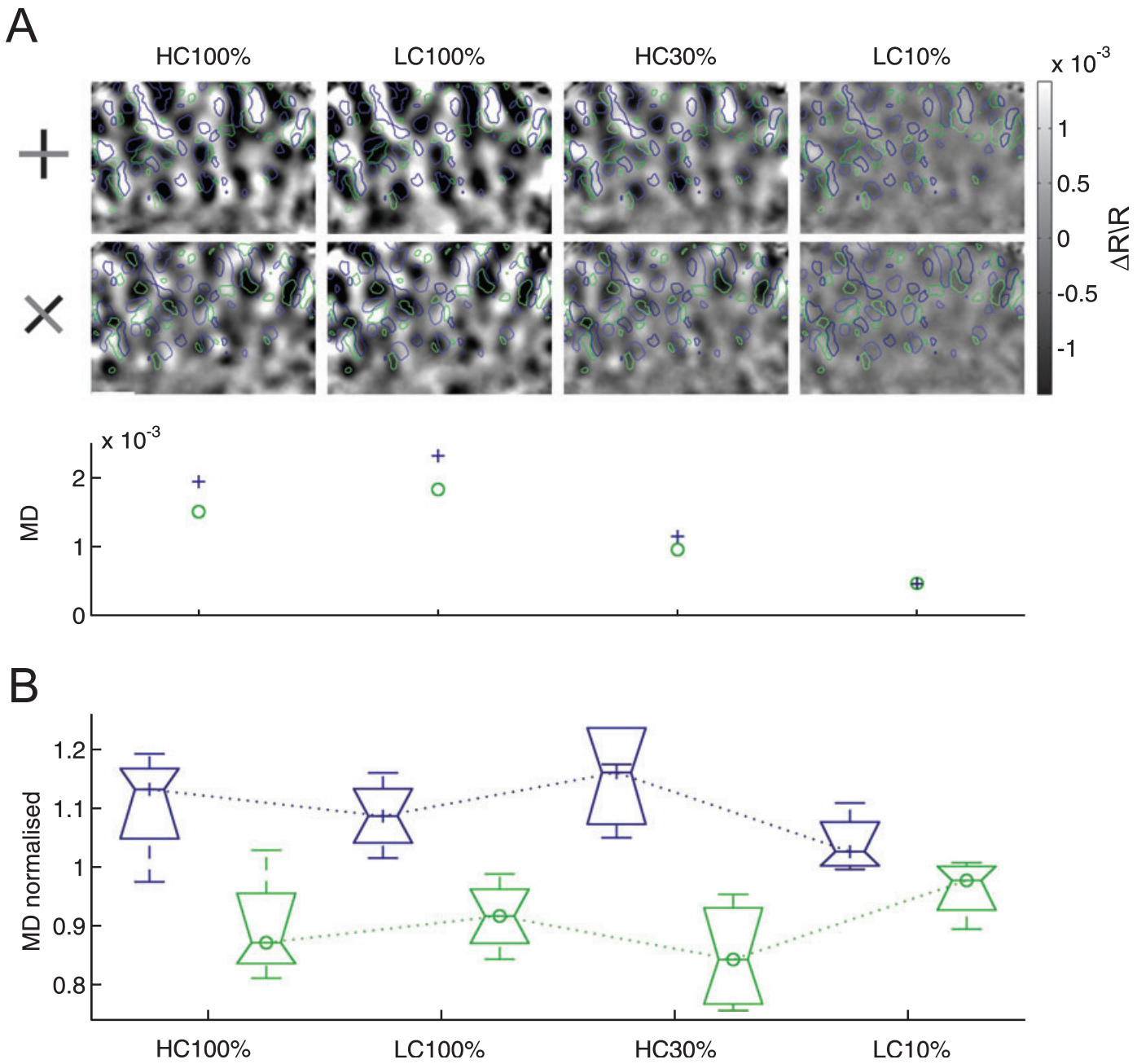

FIG. 3. Effect of stimulus contrast on modulation depth (MD). (A) Time-averaged differential maps of cardinal and oblique grating orientations (see symbols at left; stimulus contrast indicated on top) and calculated MD (lower graph). Differential maps were created by subtracting orthogonal single condition maps (such as shown in Fig. 2A). Evoked patterns of activity were similar across stimulus contrast but varied across stimulus orientations [compare regions marked by contours: blue marks regions that coded for 0° (or 90°) orientation in each contrast condition; green marks areas coding for oblique orientations]. Grating contrast of 100% was measured in two independent sets of trials (22 trials of HC and 14 trials of LC, see Materials and methods and text). Colour bar indicates signal strength $\Delta R/R$. MD was computed as standard deviation of pixel values of difference images, separately for cardinal (blue, 0–90°) and oblique (green, −45 to 45°) orientations. Only reliably responding pixels, as marked by contours, were considered. The gradual decline of MD with contrast was highly significant across experiments [MD decrease from 100% to 30%: $P = 2.9E{-}09$, $n = 9$ cases (one of the 10 cases showed no reliable preference to oblique orientation rendering it inappropriate for this comparison); from 100% to 10%: $P = 0.0001$, $n = 4$; from 30% to 10%: $P = 0.0003$, $n = 4$; Wilcoxon rank-sum tested on MD values normalized for each animal to the mean of all values]. (B) MD as a function of stimulus orientation. To allow for comparison between cardinal vs. oblique MDs across different experiments, values were normalized to the average MD across orientations, separately for each contrast condition. Medians across four experiments are depicted, lines within boxes mark lower quartile, median and upper quartile values.

Oblique orientations evoke less MD than cardinal orientations

For high-contrast gratings the single condition maps shown in Fig. 2A confirmed the principal organization of orientation-selective neurons grouped in functional clusters that revealed complementary patterns evoked by orthogonal orientations. In Fig. 3 we present differential images for all measured stimulus contrasts. As expected, a decrease in stimulus contrast (left to right) produced weaker response amplitudes, as can be inferred by decreasing 'contrast' within the images. However, both 30% and 10% contrast conditions evoked similar patterns compared with stimuli of 100% contrast of the same

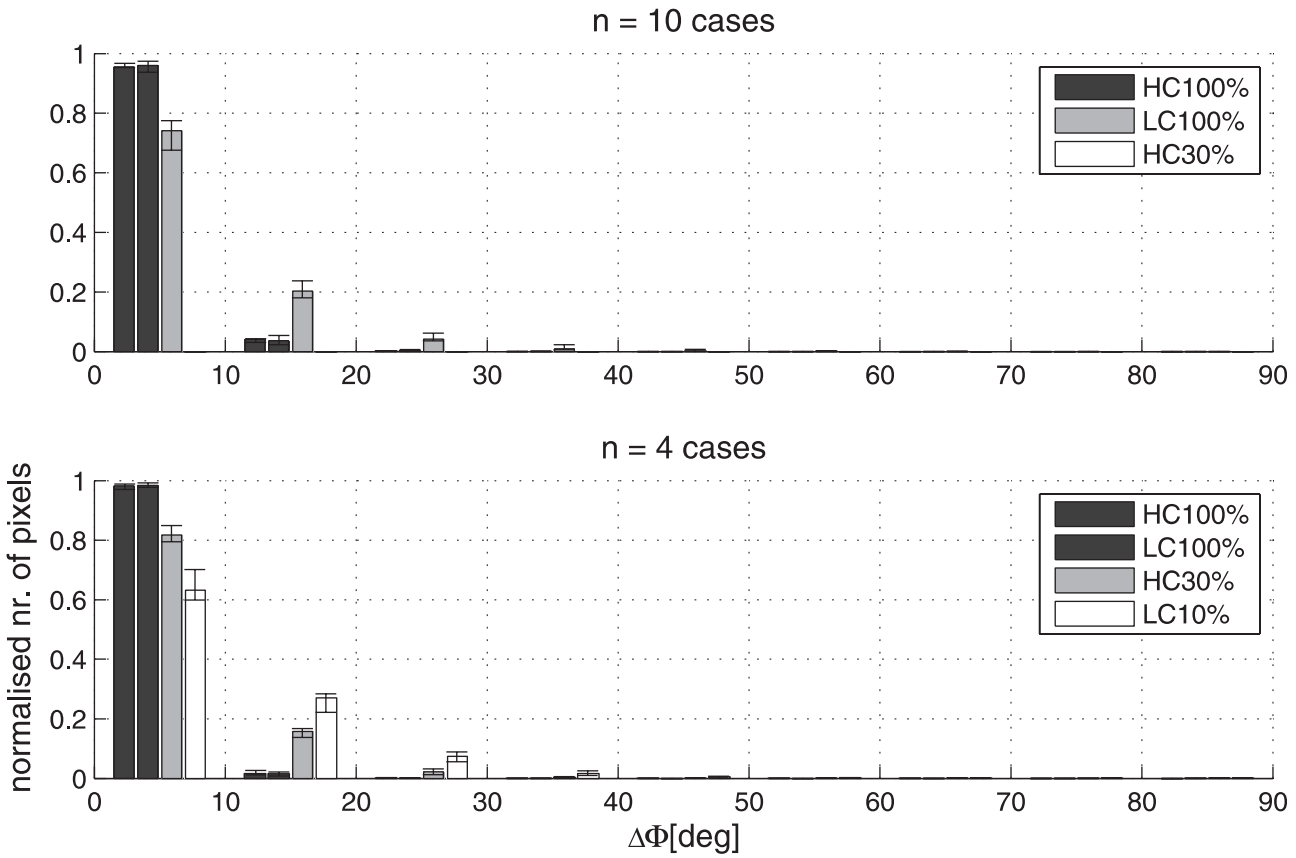

FIG. 4. OM stability. Similarities between OMs were verified on a pixel-by-pixel basis. OMs for each of the 100% contrast sets were nearly identical (compare the two black bars referring to 100% contrast conditions recorded in independent HC and LC trials). Comparison of OMs obtained with 100% and 30% contrast gratings (upper graph, $n = 10$ experiments) showed that ~80% of the pixels revealed stable orientation preference. Only a small fraction of pixels changed their tuning more than 20°. The same conclusion holds for 10% contrast conditions (lower graph, four experiments based on smaller ROIs, see text).

orientation [overlaid contours depict regions coding for cardinal (blue) and oblique (green) orientations].

Note that 100% contrast conditions were measured twice (two left columns). Instead of presenting all stimuli in a large trial at once, alternating trials consisted of two subsets of 'high-contrast' ('HC', 100% plus 30%) and 'low-contrast' conditions ('LC', 100% plus 10%). Limiting trial length effectively: (i) reduced intra-trial variance caused by slow drifts in baseline related to physiological fluctuations; and (ii) allowed a more frequent access to the preparation. Moreover, the presence of 100% contrast gratings in two independent stimulus sets served as a reference and therefore as a valuable control of the reproducibility of recordings during the entire experiment. As can be seen in Fig. 3A, the maps measured with 100% stimulus contrast in HC and LC sets were almost identical (see also Figs 1 and 4), confirming both the stable quality of the recordings and the efficiency of the applied GIF procedure.

Corresponding to the decrease in response amplitudes with lower contrasts, we found a significant decrease in MD, here simply calculated as the standard deviation of differential image pixel values, computed separately for regions coding for cardinal and oblique orientations and for each contrast (Fig. 3A).

Figure 3B presents the summary of MD values obtained for the four cases that showed reliable responses across all contrast conditions, here the values were normalized for each animal and contrast condition. The MD revealed consistently lower values in oblique compared with cardinal OMs. This was significant for 100% and 30% contrast conditions ($P = 0.05$ for HC100%, $P = 0.024$ for LC100%, $P = 0.002$ for HC30%, $n = 9$, Wilcoxon rank-sum test). Due to the decrease in signal-to-noise ratio for low contrasts, slightly higher P-values were observed for 10% contrast ($P = 0.057$, $n = 4$, Wilcoxon rank-sum test). Thus, orientation selectivity within large populations of neurons coding for cardinal orientations was higher than for neuronal populations coding for oblique orientations.

Contrast independence of the cortical oblique effect

To test whether each pixel maintained its preferred orientation tuning throughout the various contrast measurements, we used the mean of the OMs obtained with high-contrast stimuli (HC/LC 100%) as a reference map and calculated how many pixels changed their orientation preference in different contrast conditions. Both 100% contrast maps were highly similar to their mean reference map (and thus to each other), proving the correct choice of ROIs and the high quality of the recordings. Comparing 100% and 30% contrast over all experiments (Fig. 4, upper graph, $n = 10$ cases), we found that pixels maintained their preferred orientation mostly within 10°. This similarity decreased only slightly for lower contrasts (Fig. 4, lower graph, $n = 4$ cases). Thus, the general layout of the OMs was preserved over the entire range of stimulus contrasts.

Having confirmed that the OMs were stable across contrasts, we finally investigated whether the map layout indeed revealed the well-known cortical oblique effect. Figure 5A illustrates the distribution of pixel counts according to preferred orientations (the same example as

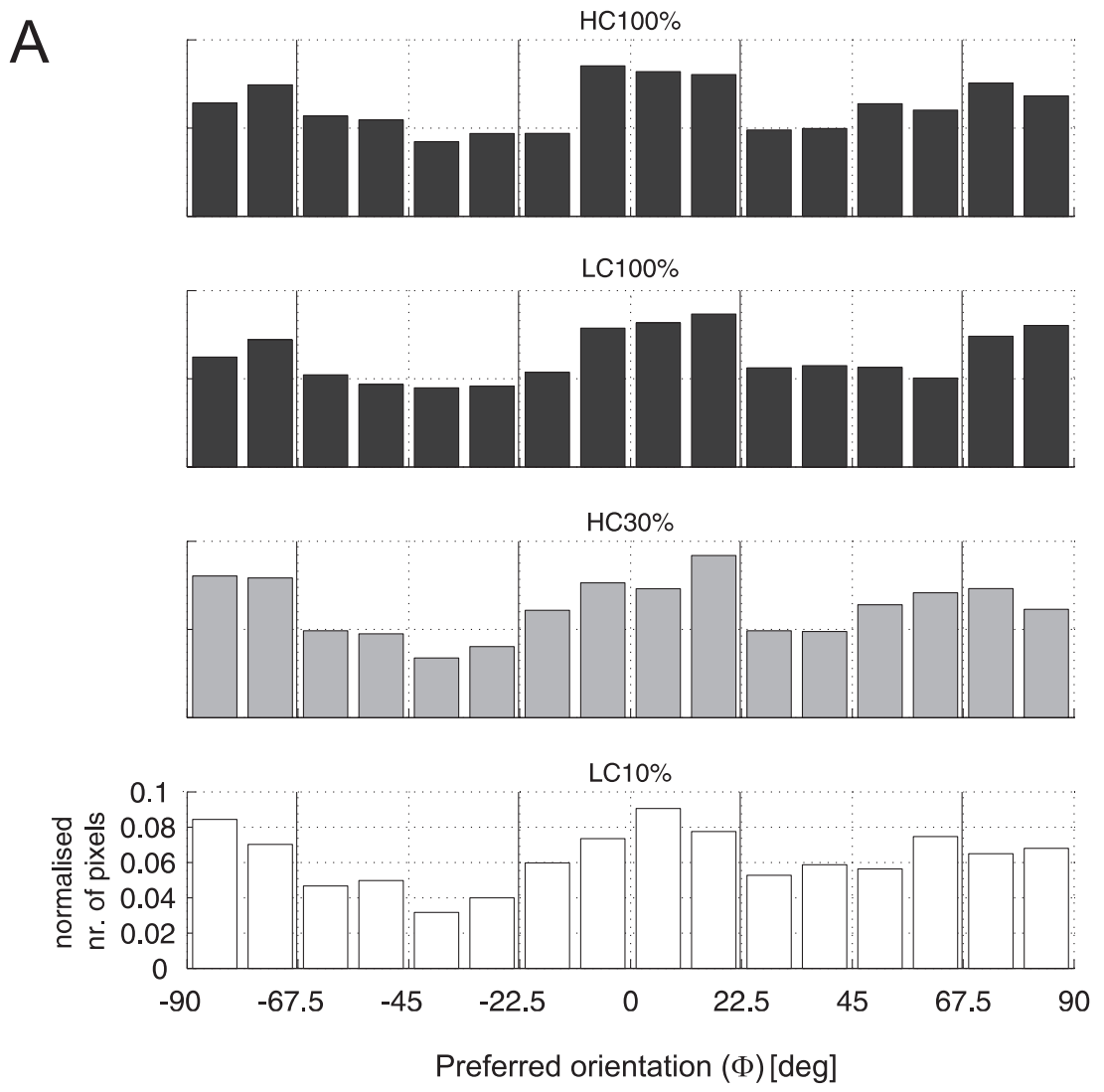

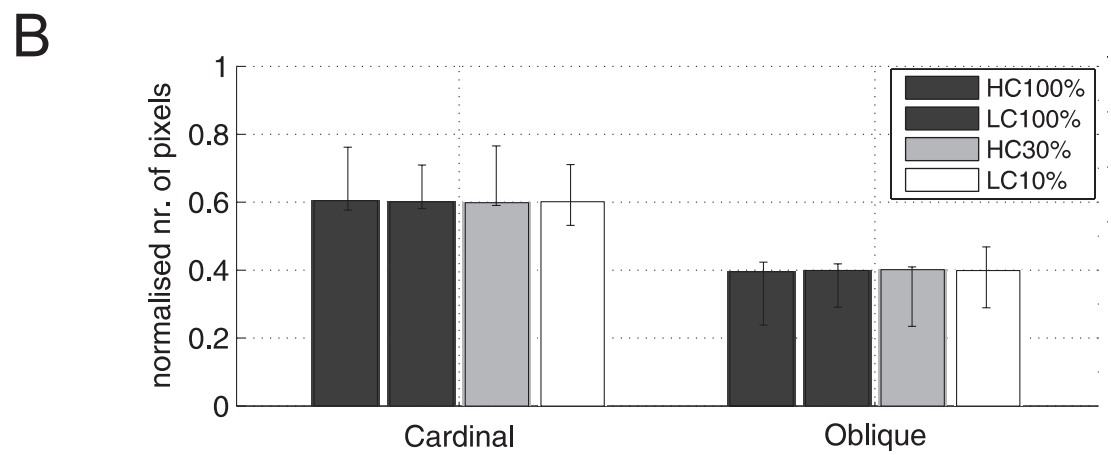

FIG. 5. Contrast independence of the cortical oblique effect. Histograms show relative numbers of pixels coding for a particular stimulus orientation with reproducibility $r(k) > 0.2$ (see Materials and methods). (A) Establishing the oblique effect across all contrasts for the example presented in Fig. 1D–F and Figs 2 and 3. The oblique effect was revealed by 61% overrepresentation of pixels coding for cardinal orientations. Black vertical lines separate the range (in angle) of cardinal and oblique orientations. (B) Significance of the oblique effect across different experiments. Histograms of preferred pixel orientations were calculated separately for HC100%, LC100%, HC30% and LC10% conditions, and depicted as the ratio of the total number of significantly coding pixels. The histogram shows the medians of four experiments, in which the reliably orientation-tuned cortical area in 10% contrast conditions exceeded 5000 image pixels. Whiskers indicate the lowest and highest scores. The oblique effect across all contrasts was characterized by 60% overrepresentation of cardinally coding pixels (range: 55–74%). Over all experiments ($n = 10$), in 100% and 30% contrast conditions (including larger ROIs), 63% (range: 53–95%) of the total pixels were assigned to cardinal orientation. We found no systematic bias between horizontal and vertical representations (2% in Coppola *et al.*, 1998a).

shown in Figs 1D–F, 2 and 3). The distribution peaks at cardinal orientations across all stimulus contrasts. Thus, the cortical oblique effect was established by an overrepresentation of pixels coding for orientations of 0 and 90° from high contrasts down to threshold levels.

The stability of the oblique effect was verified across all experiments ($n = 10$) for 100% and 30% contrast conditions, and separately for experiments in which responses were detected across the full range of stimulus contrasts ($n = 4$). The median percentage of pixels representing cardinal orientations was 63% in larger ROIs, containing pixels reliably coding across 100% to 30% conditions ($n = 10$ cases), and 60% as measured in smaller ROIs (reproducibility tested across all contrast conditions, $n = 4$ experiments; Fig. 5B).

Although the total number of reliable pixels decreased with lower stimulus contrasts, we found no significant change in pixel ratio between cardinal and oblique orientations (Wilcoxon rank-sum test, $P > 0.8$; P-values were lower but still insignificant when estimated with paired tests). Thus, as summarized in Fig. 5B, the amount of pixels expressing preference for cardinal orientations was always higher than for oblique orientations, and therefore independent of grating contrast. We conclude that the stable layout of the OMs represents orientation anisotropy over the entire range of stimulus contrasts.

Robustness is higher for cardinal orientations

We finally analysed whether any differences in the reliability between cardinally and obliquely coding regions could be detected (Fig. 6). For all experiments, Fig. 6A presents the density of pixels $p(r', \Phi')$, depending on their reproducibility (r') and preferred orientation (Φ') for each contrast separately. The overrepresentation of cardinal orientations is evident in every contrast condition (see white areas of highest density), as well as the decrease in reproducibility with decreasing contrast.

In order to eliminate the bias caused by the oblique effect, the densities were normalized by the number of pixels coding for a certain orientation (Fig. 6B). The most reproducible pixels ($r' > 0.8$) show a dominant coding for cardinal orientations (upper part of the 2D histogram). Pixels denoting lower reproducibility values represented oblique orientations (see bright areas $r' \sim 0.5$ in the contour plot). Thus, the overall robustness of orientation coding was higher for cardinal orientations.

Discussion

The oblique effect, a higher sensitivity for cardinal as opposed to oblique orientations, has been addressed in many experimental and theoretical studies (Campbell *et al.*, 1966; Maffei & Campbell, 1970; Frost & Kaminer, 1975; Essock, 1982; Lasagaa & Garner, 1983; Orban *et al.*, 1984; Moskowitz & Sokol, 1985; Heeley & Timney, 1988; Furmanski & Engel, 2000; Tibber *et al.*, 2006). It is widely assumed that the functional cortical organization, including its preference for processing of cardinal orientations, is reflective of the statistics in natural images that are rich in contours parallel or perpendicular to the direction of gravitational force (Field, 1987; van der Schaaf & van Hateren, 1996; Coppola *et al.*, 1998b; but see Switkes *et al.*, 1978; Li *et al.*, 2003; Coppola & White, 2004).

In natural images, contrast varies in approximately 1–1.5 log unit range (Frazor & Geisler, 2006). Accordingly, the visual system has evolved various adaptive mechanisms providing contrast invariance across a wide range of luminance changes, spatial frequencies, spatial phase, direction of motion, and orientation (Albrecht & Hamilton, 1982; Sclar *et al.*, 1990; Albrecht & Geisler, 1991; Geisler & Albrecht, 1997; Graham & Sutter, 2000; Albrecht *et al.*, 2002; Geisler *et al.*, 2007). The specific aim of this study was to explore whether the cortical oblique effect is maintained at low stimulus contrast around response threshold.

Orientation tuning of single cells in relation to mass activation revealed by optical imaging

Optical imaging and single-cell electrophysiology are confronted with opposing problems in neuronal sampling. Optical imaging provides an overall population picture of the functional architecture across entire cortical areas but at the cost of a detailed description of the underlying single-cell properties. In contrast, single-cell studies provide such cellular resolution but often fail to obtain a conclusive, large-scale picture of neuronal activation.

Intrinsic signals reflect firing of a large number of neurons, but also include their widespread presynaptic and subthreshold postsynaptic activity in addition to suprathreshold cortical activation (Das & Gilbert, 1995; Toth *et al.*, 1996; Logothetis *et al.*, 2001; Zhan *et al.*, 2005). In addition, because the haemodynamic responses are slow compared with the underlying electrical events, subtle contrast-related changes in firing patterns cannot be detected by the optical signal. Thus, each image pixel represents time-averaged activity summed over populations of neurons at mesoscopic levels (Dinse & Jancke, 2001). Light scattering, scatter in vasculature and spread of metabolic demand underlying the haemodynamic responses limit spatial resolution. Furthermore, optical signals emphasize activation of upper cortical layers. Remarkably, however, OMs derived by optical imaging have been shown to precisely match orientation tuning of single neurons even at pinwheel centres, where a gradual change in preferred orientation across the entire depth of cortical layers converges to a precise arrangement of differently tuned neurons in close proximity (Maldonado *et al.*, 1997; Ohki *et al.*, 2006).

On the other hand, single-cell measurements inevitably provide only limited sampling within an animal and therefore often fail to demonstrate a general picture of the functional structure. Using extracellular recordings several studies found evidence for a bias in the number of neurons preferentially tuned to cardinal orientations in cats (Pettigrew *et al.*, 1968; Kalia & Whitteridge, 1973; Kennedy & Orban, 1979; Payne & Berman, 1983) and monkeys (Mansfield, 1974; De Valois *et al.*, 1982). By contrast, other extracellular recordings in these animals argued for the opposite, showing a flat distribution of preferred orientations (Campbell *et al.*, 1968; Hubel & Wiesel, 1968; Noda *et al.*, 1971; Finlay *et al.*, 1976; Wilson & Sherman, 1976; Poggio *et al.*, 1977). Contrast affects orientation selectivity differently among cell types, across cortical layers (Albrecht & Hamilton, 1982; Sclar *et al.*, 1990), with respect to preferred spatial and temporal frequencies (Albrecht, 1995; Alitto & Usrey, 2004; but see Moore *et al.*, 2005) and eccentricity (Wilson & Sherman, 1976; Poggio *et al.*, 1977). Several studies reported anisotropies in the distribution of simple and complex cells, and inhomogeneities in response amplitudes to variations in stimulus contrasts (Albus, 1975; Nelson *et al.*, 1977; Henry *et al.*, 1978; Orban & Kennedy, 1981; Payne & Berman, 1983; Tootell *et al.*, 1988). Only extensive pooling of a large data set including thousands of neurons revealed a clear overrepresentation of cardinally tuned neurons in cat primary visual cortex (Li *et al.*, 2003).

In view of the list of contrasting results, it remained uncertain whether changes in contrast may differentially influence neuronal subpopulations that code for oblique and cardinal orientations.

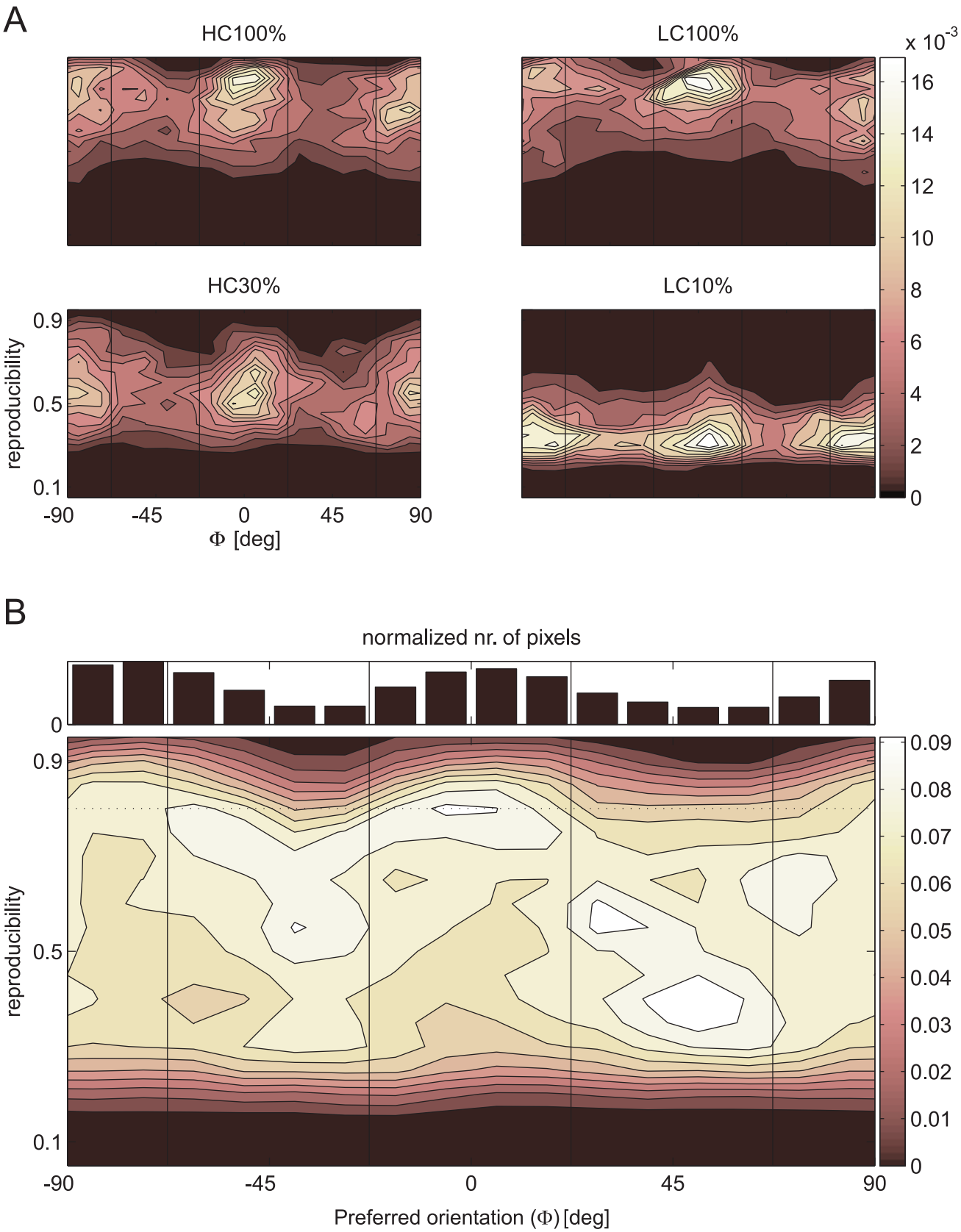

FIG. 6. Coding for cardinal orientations is more robust than for oblique. The relative number of pixels with regard to their orientation preference and reproducibility (Φ, r) is shown with a colour code. (A) For each experiment, the distribution of pixels dependent on preferred orientation was calculated for 100%, 30% and 10% contrast conditions, and normalized to the number of pixels in the image frame (mean across four experiments). (B) To account for the dominance of cardinally tuned pixels, we further normalized across orientation [$\Sigma_r\, n(\Phi, r) = 1$ for every Φ], the mean across 100%, 30% and 10% conditions is shown. In the highest reproducibility range ($r > 0.8$), most pixels code for cardinal orientations (distribution depicted with a histogram on top of the contour plot).

Stable layout of the cortical oblique effect across various contrast levels

So far only a few optical imaging studies investigated contrast dependencies of OMs systematically (Carandini & Sengpiel, 2004; Zhan *et al.*, 2005; Lu & Roe, 2007). Carandini & Sengpiel (2004) conducted experiments in cat primary visual cortex and found uniform representation of contrast. However, as their study involved fitting a model upon the pooled responses to a variety of applied contrasts and not for each stimulus contrast separately, the exact layout of the OMs at response threshold levels remained unaccounted for. The stability of orientation domains with contrast was also reported for monkey V1, implying that a presumptive underlying dominance of cardinal representation was preserved (Lu & Roe, 2007). In the present investigation we show that in the visual cortex of ferrets the cortical oblique effect for orientation persists from high contrasts down to low contrasts around response threshold. In addition, orientation selectivity, as measured by MD, and tuning robustness, as measured by the reproducibility, were consistently higher for cardinal orientations compared with oblique.

For the 100% and 30% grating contrasts we found that cortical regions representing cardinal orientations were 27% larger than for oblique orientations (n = 10 experiments). In four of the 10 experiments we detected significant responses to the 10% grating contrast, although within smaller ROIs. Still, in this condition, we found 20% more cortical area preferentially responding to cardinal orientations (white bars in Fig. 5B).

In summary, these values are well within the range of those obtained for the 100% contrast condition (compare with Fig. 3 in Coppola *et al.*, 1998b), demonstrating the constancy of the prevalence of neuronal populations involved in cardinal orientation processing irrespective of stimulus contrast.

We conclude that if there exists any contrast dependency of OM layout at response threshold levels, it must appear weaker than in optically derived mapping signals of orientation and tuning width. We also cannot rule out that the dominant areal representation of cardinal orientations, as observed with optical imaging, is the result of higher response amplitudes of neurons tuned to cardinal compared with oblique orientations. In any case, our results strongly suggest that the principal arrangement of orientation domains does not change with contrast.

Higher reliability of orientation preference in cardinally coding neurons

Our data also indicate that the most reliably responding pixels were coding for cardinal orientations. At the single-cell level it is known that the variance of synaptic activity increases with decreasing contrast (Anderson *et al.*, 2000; Finn *et al.*, 2007). Our results for low contrasts indicate additional differences in variance between obliquely and cardinally tuned neurons.

Such orientation-dependent variability at early cortical processing stages should have an impact on orientation-detection thresholds (Campbell & Kulikowski, 1966; Mitchell *et al.*, 1967). Indeed, parallel functional magnetic resonance imaging (fMRI) and behavioural experiments have confirmed an analogue correspondence: fMRI responses in V1 were larger for orientations that yielded better perceptual performance (Furmanski & Engel, 2000). Lower detection thresholds for cardinal orientations observed in behavioural studies mean that recognition of cardinal orientations at lowest stimulus contrasts was above chance while the detection of oblique stimuli at these contrasts was still random. These behavioural results are consistent with our neurophysiological observation that cardinal stimuli evoked more reliable responses even at the lowest stimulus contrasts.

Oblique orientation effect in higher visual cortical areas – stimulus complexity may matter

Using gratings of lower spatial frequencies in a psychophysical study, Zemon *et al.* (1993) reported that the oblique effect diminishes at suprathreshold levels, contradicting earlier results obtained for behavioural judgements (Essock, 1982; Lasagaa & Garner, 1983). The authors then speculated that neuronal excitatory and inhibitory interaction along the visual pathway might lead to an adjustment in the gain to compensate for the lower sensitivity to oblique orientations. By contrast, optical imaging experiments conducted in visual areas further downstream demonstrated that the oblique orientation effect is even stronger compared with the early visual cortex (Huang *et al.*, 2006; Xu *et al.*, 2006), suggesting that feedback projections from higher-order cortical areas enhance the oblique effect through cooperative mechanisms (Liang *et al.*, 2007). Surprisingly, with the use of more complex stimuli such as natural scenes, which contain broadband spatial frequencies, it has been demonstrated that the oblique effect diminishes or could be even turned into a 'horizontal effect' (Essock *et al.*, 2003; Hansen & Essock, 2006). Thus, it remains controversial to what extent the oblique effect depends on spatial and temporal frequencies (De Valois *et al.*, 1982; Coletta *et al.*, 1993; Pointer, 1996; Westheimer, 2003).

So far, most physiological studies – including ours – that investigated cortical OMs were obtained by using full-screen gratings that uniformly covered the visual field and had 'optimal' spatio-temporal frequencies. In future work, it will be interesting to see how complex stimulation (Heinrich *et al.*, 2008) together with local contrast variations and more time-critical visual events might influence the oblique effect (Essock *et al.*, 2003) as well as the mapping of orientation (Jancke, 2000; Dragoi *et al.*, 2002). In particular, more complex stimulation may involve adaptive dynamics leading to changes in the cortical functional architecture on short time scales (Macé *et al.*, 2005; Yao *et al.*, 2007; Onat *et al.*, 2008).

Supporting information

Additional supporting information may be found in the online version of this article:

Fig. S1. Single condition maps derived from generalized indicator function (GIF) analysis.

Appendix S1. Setting appropriate filter size: comparison of high-pass filtered images with images derived by GIF analysis.

Appendix S2. Statistical evaluation of orientation maps.

Please note: Wiley-Blackwell are not responsible for the content or functionality of any supporting materials supplied by the authors. Any queries (other than missing material) should be directed to the corresponding author for the article.

Acknowledgements

This work was financed by Bundesministerium für Bildung und Forschung, BMBF (D.J.), Deutsche Forschungsgemeinschaft, SFB Neurovision 509 (C.D., K.-P.H.), International Graduate School of Neuroscience (A.G.-B.). We thank Alexandra Nagetusch for help during the experiments, and Stefan Dobers and the mechanical shop for excellent technical support. We thank Benedict Ng, Marek Barwiński and John Lipinski for helpful comments on the manuscript, and two anonymous reviewers for constructive criticism.

Abbreviations

fMRI, functional magnetic resonance imaging; GIF, generalized indicator function; HC, trials consisting of 100% and 30% contrast stimuli; LC, trials consisting of 100% and 10% contrast stimuli; MD, modulation depth; OMs, orientation maps; PCA, principal component analysis; ROI, region of interest.

References

Albrecht, D.G. (1995) Visual cortex neurons in monkey and cat: effect of contrast on the spatial and temporal phase transfer function. *Vis. Neurosci.*, **12**, 1191–1210.

Albrecht, D.G. & Geisler, W.S. (1991) Motion selectivity and the contrast-response function of simple cells in the visual cortex. *Vis. Neurosci.*, **7**, 531–546.

Albrecht, D.G. & Hamilton, D.B. (1982) Striate cortex of monkey and cat: contrast response function. *J. Neurophysiol.*, **48**, 217–237.

Albrecht, D.G., Geisler, W.S., Frazor, R.A. & Crane, A.M. (2002) Visual cortex neurons of monkeys and cats: temporal dynamics of the contrast response function. *J. Neurophysiol.*, **88**, 888–913.

Albus, K. (1975) A quantitative study of the projection area of the central and the paracentral visual field in area 17 of the cat. I. The precision of the topography. *Exp. Brain Res.*, **24**, 159–179.

Alitto, H.J. & Usrey, W.M. (2004) Influence of contrast on orientation and temporal frequency tuning in ferret primary visual cortex. *J. Neurophysiol.*, **91**, 2797–2808.

Anderson, J.S., Lampl, L., Gillespie, D. & Ferster, D. (2000) The contribution of noise to contrast invariance of orientation tuning in cat visual cortex. *Science*, **290**, 1968–1971.

Appelle, S. (1972) Perception and discrimination as a function of stimulus orientation: the 'oblique effect' in man and animals. *Psychol. Bull.*, **78**, 266–278.

Blasdel, G.G. & Salama, G. (1986) Voltage-sensitive dyes reveals a modular organization in the monkey striate cortex. *Nature*, **321**, 579–585.

Bonhoeffer, T. & Grinvald, A. (1991) Iso-orientation domains in cat visual cortex are arranged in pinwheel-like patterns. *Nature*, **353**, 429–431.

Bonhoeffer, T. & Grinvald, A. (1993) The layout of iso-orientation domains in area 18 of cat visual cortex: optical imaging reveals a pinwheel-like organization. *J. Neurosci.*, **13**, 4157–4180.

Bosking, W.H., Zhang, Y., Schofield, B. & Fitzpatrick, D. (1997) Orientation selectivity and arrangement of horizontal connections in tree shrew striate cortex. *J. Neurosci.*, **17**, 2112–2127.

Campbell, F.W. & Kulikowski, J.J. (1966) Orientational selectivity of the human visual system. *J. Physiol.*, **187**, 437–445.

Campbell, F.W., Kulikowski, J.J. & Levinson, J. (1966) The effect of orientation on the visual resolution of gratings. *J. Physiol.*, **187**, 427–436.

Campbell, F.W., Cleland, B.G., Cooper, G.F. & Enroth-Cugell, C. (1968) The angular selectivity of visual cortical cells to moving gratings. *J. Physiol.*, **198**, 237–250.

Carandini, M. & Sengpiel, F. (2004) Contrast invariance of functional maps in cat primary visual cortex. *J. Vis.*, **4**, 130–143.

Chapman, B. & Bonhoeffer, T. (1998) Overrepresentation of horizontal and vertical orientation preferences in developing ferret area 17. *Proc. Natl Acad. Sci. USA*, **95**, 2609–2614.

Coletta, N.J., Segu, P. & Tiana, C.L. (1993) An oblique effect in parafoveal motion perception. *Vision Res.*, **33**, 2747–2756.

Coppola, D.M. & White, L.E. (2004) Visual experience promotes the isotropic representation of orientation preference. *Vis. Neurosci.*, **21**, 39–51.

Coppola, D.M., White, L.E., Fitzpatrick, D. & Purves, D. (1998a) Unequal representation of cardinal and oblique contours in ferret visual cortex. *Proc. Natl Acad. Sci. USA*, **95**, 2621–2623.

Coppola, D.M., Purves, H.R., McCoy, A.N. & Purves, D. (1998b) The distribution of oriented contours in the real world. *Proc. Natl Acad. Sci. USA*, **95**, 4002–4006.

Das, A. & Gilbert, C.D. (1995) Long-range horizontal connections and their role in cortical reorganization revealed by optical recording of cat primary visual cortex. *Nature*, **375**, 780–784.

De Valois, R.L., Yund, E.W. & Hepler, N. (1982) The orientation and direction selectivity of cells in macaque visual cortex. *Vision Res.*, **22**, 531–544.

Dinse, H.R. & Jancke, D. (2001) Time-variant processing in V1: from microscopic (single cell) to mesoscopic (population) levels. *TINS*, **24**, 203–205.

Dragoi, V., Sharma, J., Miller, E.K. & Sur, M. (2002) Dynamics of neuronal sensitivity in visual cortex and local feature discrimination. *Nat. Neurosci.*, **5**, 883–891.

Essock, E.A. (1982) Anisotropies of perceived contrast and detection speed. *Vision Res.*, **22**, 1185–1191.

Essock, E.A., DeFord, J.K., Hansen, B.C. & Sinai, M.J. (2003) Oblique stimuli are seen best (not worst!) in naturalistic broad-band stimuli: a horizontal effect. *Vision Res.*, **43**, 1329–1335.

Ferster, D. & Miller, K.D. (2000) Neural mechanisms of orientation selectivity in the visual cortex. *Annu. Rev. Neurosci.*, **23**, 441–471.

Field, D.J. (1987) Relations between the statistics of natural images and the response properties of cortical cells. *J. Opt. Soc. Am. A*, **4**, 2379–2394.

Finlay, B.L., Schiller, P.H. & Volman, S.F. (1976) Meridional differences in orientation sensitivity in monkey striate cortex. *Brain Res.*, **105**, 350–352.

Finn, I.M., Priebe, N.J. & Ferster, D. (2007) The emergence of contrast-invariant orientation tuning in simple cells of cat visual cortex. *Neuron*, **54**, 137–152.

Frazor, R.A. & Geisler, W.S. (2006) Local luminance and contrast in natural images. *Vision Res.*, **46**, 1585–1598.

Frost, B.J. & Kaminer, J.J. (1975) The orientation anisotropy and orientation constancy: a visual evoked potential study. *Perception*, **1**, 51–58.

Furmanski, C.S. & Engel, S.A. (2000) An oblique effect in human primary visual cortex. *Nat. Neurosci.*, **3**, 535–536.

Geisler, W.S. & Albrecht, D.G. (1997) Visual cortex neurons in monkeys and cats: detection, discrimination, and identification. *Vis. Neurosci.*, **14**, 897–919.

Geisler, W.S., Albrecht, D.G. & Crane, A.M. (2007) Responses of neurons in primary visual cortex to transient changes in local contrast and luminance. *J. Neurosci.*, **27**, 5063–5067.

Graham, N. & Sutter, A. (2000) Normalization: contrast-gain control in simple (Fourier) and complex (non-Fourier) pathways of pattern vision. *Vision Res.*, **40**, 2737–2761.

Hansen, B.C. & Essock, E.A. (2006) Anisotropic local contrast normalization: the role of stimulus orientation and spatial frequency bandwidths in the oblique and horizontal effect perceptual anisotropies. *Vision Res.*, **46**, 4398–4415.

Heeger, D.J. (1992) Normalization of cell responses in cat striate cortex. *Vis. Neurosci.*, **9**, 181–197.

Heeley, D.W. & Timney, B. (1988) Meridional anisotropies of orientation discrimination for sine wave gratings. *Vision Res.*, **28**, 337–344.

Heinrich, S.P., Aertsen, A. & Bacha, M. (2008) Oblique effects beyond low-level visual processing. *Vision Res.*, **48**, 809–818.

Henry, G.H., Goodwin, A.W. & Bishop, P.O. (1978) Spatial summation of responses in receptive fields of single cells in cat striate cortex. *Exp. Brain Res.*, **32**, 245–266.

Holub, R.A. & Morton-Gibson, M. (1981) Response of visual cortical neurons of the cat to moving sinusoidal gratings: response-contrast functions and spatiotemporal interactions. *J. Neurophysiol.*, **91**, 2797–2808.

Howard, I.P. & Templeton, W.B. (1966) *Human Spatial Orientation*. Wiley, London.

Huang, L., Shou, T., Chen, X., Yu, H., Sun, C. & Liang, Z. (2006) Slab-like functional architecture of higher order cortical area 21a showing oblique effect of orientation preference in the cat. *Neuroimage*, **32**, 1365–1374.

Hubel, D.H. & Wiesel, T.N. (1968) Receptive fields and functional architecture of monkey striate cortex. *J. Physiol.*, **195**, 215–243.

Hubel, D.H. & Wiesel, T.N. (1974) Sequence regularity and geometry of orientation columns in the monkey striate cortex. *J. Comp. Neurol.*, **158**, 267–293.

Hübener, M., Shoham, D., Grinvald, A. & Bonhoeffer, T. (1997) Spatial relationships among three columnar systems in cat area 17. *J. Neurosci.*, **17**, 9270–9284.

Hupfeld, D., Distler, C. & Hoffmann, K.-P. (2006) Motion perception deficits in albino ferrets (*Mustela putorius furo*). *Vision Res.*, **46**, 2941–2948.

Jancke, D. (2000) Orientation formed by a spot's trajectory: a two-dimensional population approach in primary visual cortex. *J. Neurosci.*, **20**, RC86.

Kalia, M. & Whitteridge, D. (1973) The visual areas in the splenial sulcus of the cat. *J. Physiol.*, **232**, 275–283.

Kennedy, H. & Orban, G.A. (1979) Preferences for horizontal or vertical orientation in cat visual cortical neurons. *J. Physiol.*, **296**, 61–62.

Lasagaa, M.I. & Garner, W.R. (1983) Effect of line orientation on various information-processing tasks. *J. Exp. Psychol. Hum. Percept. Perform.*, **9**, 215–225.

Leventhal, A.G. & Hirsch, H.V. (1975) Cortical effect of early selective exposure to diagonal lines. *Science*, **190**, 902–904.

Li, B., Peterson, M.R. & Freeman, R.D. (2003) Oblique effect: a neural basis in the visual cortex. *J. Neurophysiol.*, **90**, 204–217.

Li, Y., Fitzpatrick, D. & White, L.E. (2006) The development of direction selectivity in ferret visual cortex requires early visual experience. *Nat. Neurosci.*, **9**, 576–581.

Liang, Z., Shen, W. & Shou, T. (2007) Enhancement of oblique effect in the cat's primary visual cortex via orientation preference shifting induced by excitatory feedback from higher-order cortical area 21a. *Neuroscience*, **145**, 377–383.
Logothetis, N.K., Pauls, J., Augath, M., Trinath, T. & Oeltermann, A. (2001) Neurophysiological investigation of the basis of the fMRI signal. *Nature*, **412**, 150–157.
Lu, H.D. & Roe, A.W. (2007) Optical imaging of contrast response in macaque monkey V1 and V2. *Cereb. Cortex*, **17**, 2675–2695.
Macé, M.J., Thorpe, S.J. & Fabre-Thorpe, M. (2005) Rapid categorization of achromatic natural scenes: how robust at very low contrasts? *Eur. J. Neurosci.*, **21**, 2007–2018.
Maffei, L. & Campbell, F.W. (1970) Neurophysiological localization of the vertical and horizontal visual coordinates in man. *Science*, **167**, 386–387.
Maldonado, P.E., Gödecke, I., Gray, C.M. & Bonhoeffer, T. (1997) Orientation selectivity in pinwheel centers in cat striate cortex. *Science*, **276**, 1551–1555.
Mansfield, R.J.W. (1974) Neural basis of orientation perception in primate vision. *Science*, **186**, 1133–1135.
Mitchell, D.E., Freeman, R.D. & Westheimer, G. (1967) Effect of orientation on the modulation sensitivity for interference fringes on the retina. *J. Opt. Soc. Am.*, **57**, 246–249.
Moore, B.D. IV, Alitto, H.J. & Usrey, W.M. (2005) Orientation tuning, but not direction selectivity, is invariant to temporal frequency in primary visual cortex. *J. Neurophysiol.*, **94**, 1336–1345.
Moskowitz, A. & Sokol, S. (1985) Effect of stimulus orientation on the latency and amplitude of the VEP. *Invest. Ophthalmol. Vis. Sci.*, **26**, 246–248.
Müller, T., Stetter, M., Hübener, M., Sengpiel, F., Bonhoeffer, T., Gödecke, I., Chapman, B., Löwel, S. & Obermayer, K. (2000) An analysis of orientation and ocular dominance patterns in the visual cortex of cats and ferrets. *Neural Comput.*, **12**, 2573–2595.
Nelson, J.I., Kato, H. & Bishop, P.O. (1977) Discrimination of orientation and position disparities by binocularly activated neurons in cat striate cortex. *J. Neurophysiol.*, **40**, 260–283.
Noda, H., Freeman, R.B. Jr & Creutzfeldt, O.D. (1971) Neuronal responses in the visual cortex of awake cats to stationary and moving targets. *Exp. Brain Res.*, **12**, 389–405.
Ohki, K., Chung, S., Kara, P., Hübener, M., Bonhoeffer, T. & Reid, R.C. (2006) Highly ordered arrangement of single neurons in orientation pinwheels. *Nature*, **442**, 925–928.
Onat, S., König, P. & Jancke, D. (2008) Long-range interactions in natural scene processing revealed by voltage-sensitive dye imaging across primary visual cortex. *Soc. Neurosci. Abstr.*, 163.8.
Orban, G.A. & Kennedy, H. (1981) The influence of eccentricity on receptive field types and orientation selectivity in areas 17 and 18 of the cat. *Brain Res.*, **208**, 203–208.
Orban, G.A., Vandenbussche, E. & Vogels, R. (1984) Human orientation discrimination tested with long stimuli. *Vision Res.*, **24**, 121–128.
Palmer, S.E. & Miller, K.D. (2007) Effects of inhibitory gain and conductance fluctuations in a simple model for contrast-invariant orientation tuning in cat V1. *J. Neurophysiol.*, **98**, 63–78.
Payne, B.R. & Berman, N. (1983) Functional organization of neurons in cat striate cortex: variations in preferred orientation and orientation selectivity with receptive-field type, ocular dominance, and location in visual-field map. *J. Neurophysiol.*, **49**, 1051–1072.
Pettigrew, J.D., Nikara, T. & Bishop, P.O. (1968) Responses to moving slits by single units in cat striate cortex. *Exp. Brain Res.*, **6**, 373–390.
Poggio, G.F., Doty, R.W.J. & Talbot, W.H. (1977) Foveal striate cortex of behaving monkey: single-neuron responses to square-wave gratings during fixation of gaze. *J. Neurophysiol.*, **40**, 1369–1391.
Pointer, J.S. (1996) Evidence of a global oblique effect in human extrafoveal vision. *Perception*, **25**, 523–530.
Ratzlaff, E.H. & Grinvald, A. (1991) A tandem-lens epifluorescence macroscope: hundred-fold brightness advantage for wide-field imaging. *J. Neurosci. Methods*, **36**, 127–137.
Rose, D. & Blakemore, C. (1974) An analysis of orientation selectivity in the cat's visual cortex. *Exp. Brain Res.*, **20**, 1–17.
van der Schaaf, A. & van Hateren, J.H. (1996) Modelling the power spectra of natural images: statistics and information. *Vision Res.*, **36**, 2759–2770.
Sclar, G. & Freeman, R.D. (1982) Orientation selectivity in the cat's striate cortex is invariant with stimulus contrast. *Exp. Brain Res.*, **46**, 457–461.
Sclar, G., Maunsell, J.H. & Lennie, P. (1990) Coding of image contrast in central visual pathways of the macaque monkey. *Vision Res.*, **30**, 1–10.
Shapley, R.M., Johnson, E.N., Hawken, M.J. & Kang, K. (2002) Orientation selectivity and stimulus contrast in macaque V1. *Soc. Neurosci. Abstr.*, 720.6.
Skottun, B.C., Bradley, A., Sclar, G., Ohzawa, I. & Freeman, R.D. (1987) The effects of contrast on visual orientation and spatial frequency discrimination: a comparison of single cells and behavior. *J. Neurophysiol.*, **57**, 773–786.
Swindale, N.V. (1998) Orientation tuning curves: empirical description and estimation of parameters. *Biol. Cybern.*, **78**, 45–56.
Switkes, E., Mayer, M.J. & Sloan, J.A. (1978) Spatial frequency analysis of the visual environment: anisotropy and the carpentered environment hypothesis. *Vision Res.*, **18**, 1393–1399.
Tibber, M.S., Guedes, A. & Shepherd, A.J. (2006) Orientation discrimination and contrast detection thresholds in migraine for cardinal and oblique angles. *Invest. Ophthalmol. Vis. Sci.*, **47**, 5599–5604.
Tootell, R.B.H., Hamilton, S.L. & Switkes, E. (1988) Functional anatomy of macaque striate cortex. IV. Contrast and magno-parvo streams. *J. Neurosci.*, **8**, 1594–1609.
Toth, L.J., Rao, S.C., Kim, D.S., Somers, D. & Sur, M. (1996) Subthreshold facilitation and suppression in primary visual cortex revealed by intrinsic signal imaging. *Proc. Natl Acad. Sci. USA*, **93**, 9869–9874.
Wang, G., Ding, S. & Yunokuchi, K. (2003) Representation of cardinal contour overlaps less with representation of nearby angles in cat visual cortex. *J. Neurophysiol.*, **90**, 3912–3920.
Westheimer, G. (2003) Meridional anisotropy in visual processing: implications for the neural site of the oblique effect. *Vision Res.*, **43**, 2281–2289.
Wilcoxon, F. (1945) Individual comparisons by ranking methods. *Biometrics Bull.*, **1**, 80–83.
Wilson, J.R. & Sherman, S.M. (1976) Receptive-field characteristics of neurons in cat striate cortex: changes with visual field eccentricity. *J. Neurophysiol.*, **39**, 512–533.
Xu, X., Bosking, W.H., White, L.E., Fitzpatrick, D. & Casagrande, V.A. (2005) Functional organization of visual cortex in the prosimian bush baby revealed by optical imaging of intrinsic signals. *J. Neurophysiol.*, **94**, 2748–2762.
Xu, X., Collins, C.E., Khaytin, I., Kaas, J.H. & Casagrande, V.A. (2006) Unequal representation of cardinal vs. oblique orientations in the middle temporal visual area. *Proc. Natl Acad. Sci. USA*, **103**, 17490–17495.
Yao, H., Shi, L., Han, F., Gao, H. & Dan, Y. (2007) Rapid learning in cortical coding of visual scenes. *Nat. Neurosci.*, **10**, 772–778.
Yokoo, T., Knight, B.W. & Sirovich, L. (2001) An optimization approach to signal extraction from noisy multivariate data. *Neuroimage*, **14**, 1309–1326.
Yu, H., Farley, B.J., Jin, D.Z. & Sur, M. (2005) The coordinated mapping of visual space and response features in visual cortex. *Neuron*, **47**, 267–280.
Zemon, V., Conte, M.M. & Camisa, J. (1993) Stimulus orientation and contrast constancy. *Int. J. Neurosci.*, **69**, 143–148.
Zhan, C.A., Ledgeway, T. & Baker, C.L. Jr (2005) Contrast response in visual cortex: quantitative assessment with intrinsic optical signal imaging and neural firing. *Neuroimage*, **26**, 330–346.